Resveratrol and related stilbene derivatives induce stress granules with distinct clearance kinetics

Triana Amen[a], Anthony Guihur[b], Christina Zelent[c], Robertas Ursache[b], Jörg Wilting[c], and Daniel Kaganovich[a,d,*]

[a]Department of Experimental Neurodegeneration and [c]Department of Anatomy and Cell Biology, University Medical Center Göttingen, 37073, Goettingen, Germany; [d]1Base Pharmaceuticals, Boston, MA, 02129, USA; [b]Department of Plant Molecular Biology, Faculty of Biology and Medicine, University of Lausanne, Switzerland

ABSTRACT **Stress granules (SGs) are ribonucleoprotein functional condensates that form under stress conditions in all eukaryotic cells. Although their stress-survival function is far from clear, SGs have been implicated in the regulation of many vital cellular pathways. Consequently, SG dysfunction is thought to be a mechanistic point of origin for many neurodegenerative disorders, including amyotrophic lateral sclerosis (ALS). Additionally, SGs are thought to play a role in pathogenic pathways as diverse as viral infection and chemotherapy resistance. There is a growing consensus on the hypothesis that understanding the mechanistic regulation of SG physical properties is essential to understanding their function. Although the internal dynamics and condensation mechanisms of SGs have been broadly investigated, there have been fewer investigations into the timing of SG formation and clearance in live cells. Because the lifetime of SG persistence can be a key factor in their function and tendency toward pathological dysregulation, SG clearance mechanisms deserve particular attention. Here we show that resveratrol and its analogues piceatannol, pterostilbene, and 3,4,5,4′-tetramethoxystilbene induce G3BP-dependent SG formation with atypically rapid clearance kinetics. Resveratrol binds to G3BP, thereby reducing its protein–protein association valency. We suggest that altering G3BP valency is a pathway for the formation of uniquely transient SGs.**

Monitoring Editor
Anne Spang
University of Basel

Received: Feb 10, 2021
Revised: Jul 27, 2021
Accepted: Aug 16, 2021

INTRODUCTION

Resveratrol (*trans*-3,5,4′-trihydroxystilbene) is a naturally occurring polyphenolic compound found in many plants, including *Vaccinium* (blueberry) and *Vitis* (grape; Rimando *et al.*, 2004). Resveratrol and other stilbenes are best known for the multiple protective functions that they are thought to exert, including anti-diabetic, anti-inflammatory, anti-oxidative, and (more controversially) anti-aging activities (McCormack and McFadden, 2013; Tsai *et al.*, 2017). Resveratrol activates peroxisome proliferator-activated receptors (PPAR) and sirtuins (SIRT1 in mammalian cells, Sir2 in yeast; Howitz *et al.*, 2003; Borra *et al.*, 2005); it can induce apoptosis (Oi *et al.*, 2015), binds estrogen receptors, and activates mitochondrial superoxide dismutase (MnSOD; Robb and Stuart, 2014). By virtue of its involvement in these pathways, resveratrol is thought to possess anti-inflammatory, antioxidant, and anti-cancer properties and to protect the brain against ischemic stroke (Potter *et al.*, 2002; Inoue *et al.*, 2003; Robb and Stuart, 2014). Piceatannol (*trans*-3,3′,4,5′-tetrahydroxystilbene) is a hydroxylated analog and a naturally occurring metabolite of resveratrol that has similar anti-cancer activities, inhibits tyrosine kinases, induces apoptosis, and promotes astrocyte

This article was published online ahead of print in MBoC in Press (http://www.molbiolcell.org/cgi/doi/10.1091/mbc.E21-02-0066).

Author contributions: All aspects of the work composing the manuscript were carried out jointly by D.K. and T.A. C.Z., T.A., and J.W. performed transmission electron microscopy. A.G. and R.U. carried out the plant experiments.

Conflict of interests: The authors declare no conflicts of interest with regard to the investigations.

*Address correspondence to: Daniel Kaganovich (daniel.kaganovich@med.uni-goettingen.de, dan@1basepharma.com).

Abbreviation used: SG, stress granule.

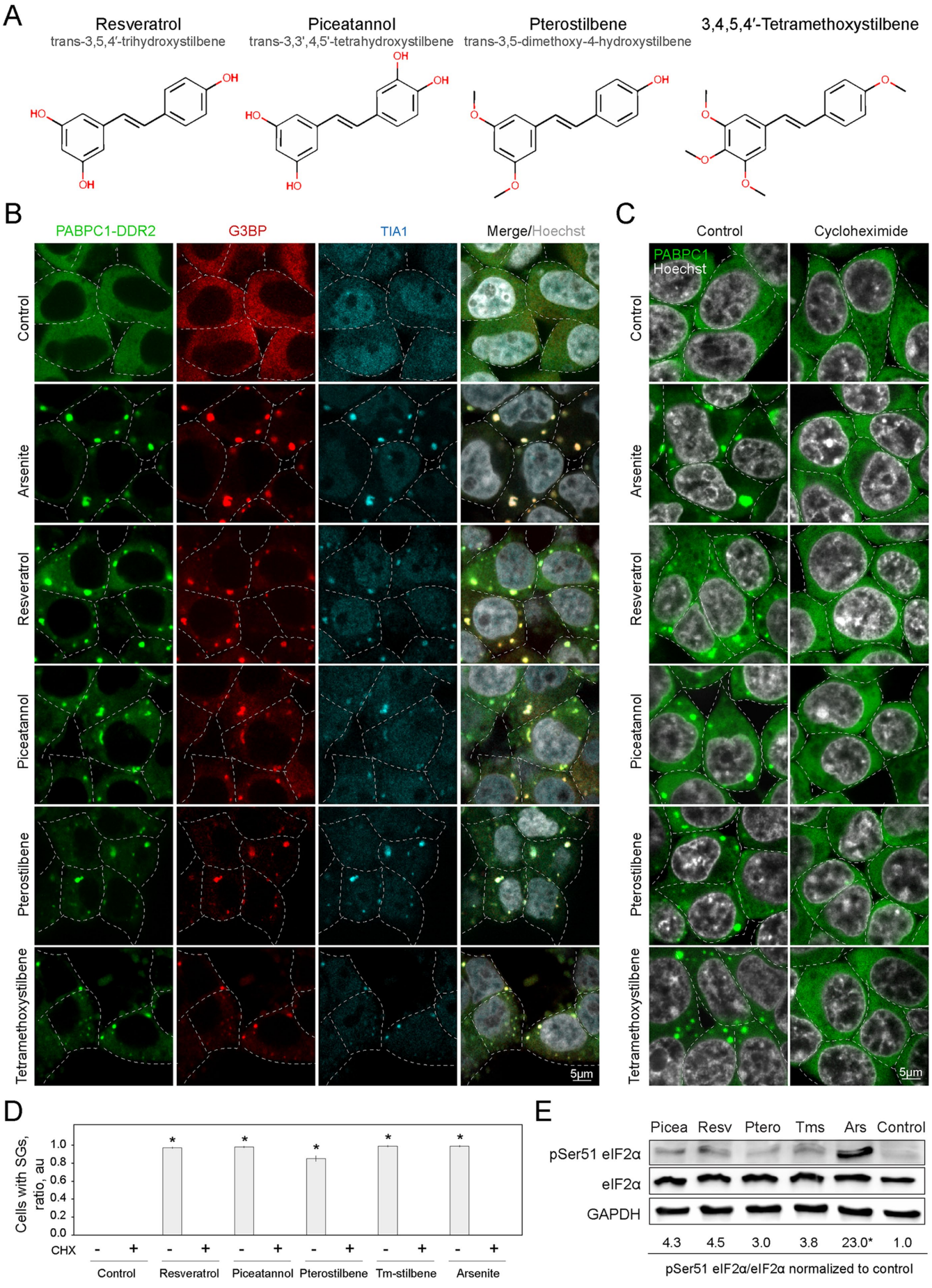
A
Resveratrol
trans-3,5,4′-trihydroxystilbene
Piceatannol
trans-3,3',4,5'-tetrahydroxystilbene
Pterostilbene
trans-3,5-dimethoxy-4-hydroxystilbene
3,4,5,4′-Tetramethoxystilbene
B
PABPC1-DDR2
G3BP
TIA1
Merge/Hoechst
Control
Arsenite
Resveratrol
Piceatannol
Pterostilbene
Tetramethoxystilbene
5μm
C
Control
Cycloheximide
PABPC1
Hoechst
Control
Arsenite
Resveratrol
Piceatannol
Pterostilbene
Tetramethoxystilbene
5μm
D
Cells with SGs, ratio, au
1.0
0.8
0.6
0.4
0.2
0.0
CHX
- + - + - + - + - + - +
Control
Resveratrol
Piceatannol
Pterostilbene
Tm-stilbene
Arsenite
E
Picea Resv Ptero Tms Ars Control
pSer51 eIF2α
eIF2α
GAPDH
4.3 4.5 3.0 3.8 23.0* 1.0
pSer51 eIF2α/eIF2α normalized to control

differentiation (Geahlen and McLaughlin, 1989; Wieder *et al.*, 2001; Potter *et al.*, 2002; Arai *et al.*, 2016). Pterostilbene (*trans*-3,5-dimethoxy-4-hydroxystilbene) is a naturally occurring dimethylated analog of resveratrol (McCormack and McFadden, 2013) that has anti-inflammatory and antioxidant effects (Lim *et al.*, 2020). The synthetic resveratrol derivative 3,4,5,4′-tetramethoxystilbene exhibits anti-cancer activities (Kim *et al.*, 2002; Fan *et al.*, 2015; Dusek *et al.*, 2019). Stilbenes are referred to as stress metabolites, since some plants up-regulate their synthesis upon infection and stress, presumably to derive benefit from their anti-fungal and other protective functions (Schmidlin *et al.*, 2008; Hasan and Bae, 2017).

Another vital stress response pathway that was initially observed in plants, but also occurs in all other eukaryotes, is the formation of stress granules (SGs): membraneless organelles that form in response to various insults, including starvation and heat stress (Anderson and Kedersha, 2006; Piotrowska *et al.*, 2010; Buchan *et al.*, 2011; Walker *et al.*, 2013; Moutaoufik *et al.*, 2014; Jevtov *et al.*, 2015; Reineke *et al.*, 2018). SG formation is thought to protect cells from stress through a variety of mechanisms, including the inhibition of pro-apoptotic kinases and antioxidant activity via the SG-resident Ras GTPase-activating protein-binding protein (G3BP1)-binding ubiquitin-specific protease 10 (USP10; Soncini *et al.*, 2001; Arimoto *et al.*, 2008; Takahashi *et al.*, 2013; Yang *et al.*, 2020). SGs also triage translation, regulate nucleocytoplasmic transport, RNA metabolism, fatty acid oxidation, among many other processes (Kedersha *et al.*, 2005, 2013; Kedersha and Anderson, 2007; Takahashi *et al.*, 2013; Panas *et al.*, 2016; Khong *et al.*, 2017; McGurk *et al.*, 2018; Zhang *et al.*, 2018a,b; Mann *et al.*, 2019; Amen and Kaganovich, 2021).

In recent years, there have been many important studies exploring the assembly mechanisms of SGs through condensation driven by multivalent interactions between SG components (Kedersha *et al.*, 2016b; Markmiller *et al.*, 2018; Sanders *et al.*, 2020; Yang *et al.*, 2020). The balance between interactions promoting and inhibiting SG formation, which often depends on a multitude of external and internal factors, determines SG assembly and dynamics (Markmiller *et al.*, 2018; Sanders *et al.*, 2020; Yang *et al.*, 2020). The main SG nucleating factors are G3BP1/2 and ubiquitin-associated protein 2-like, UBAP2L (Cirillo *et al.*, 2020; Yang *et al.*, 2020). The binding of RNA and cell cycle–associated protein 1 (Caprin1) to G3BP promotes SG formation (Kedersha *et al.*, 2016b; Markmiller *et al.*, 2018; Cirillo *et al.*, 2020; Yang *et al.*, 2020), while other factors, including USP10, Phe–Gly–Asp–Phe (FGDF) motif proteins, such as the Semliki Forest virus (nsP)3 protein, block SG formation (Panas *et al.*, 2015; Kedersha *et al.*, 2016b). Interestingly, resveratrol interacts with the main SG-nucleating component, G3BP1, preventing its interaction with USP10, which makes it a strong candidate as a SG-inducer (Oi *et al.*, 2015). Resveratrol also inhibits mammalian target of rapamycin (mTOR) kinase: another regulator of SG formation (Fournier *et al.*, 2013; Thedieck *et al.*, 2013; Park *et al.*, 2016; Sfakianos *et al.*, 2018), and protein kinase C, a kinase that regulates SG formation and physically associates with SG components (Stewart *et al.*, 1999; Slater *et al.*, 2003; Kobayashi *et al.*, 2012; Amen and Kaganovich, 2020d). Previous studies also imply that resveratrol should have the ability to trigger SG formation (Oi *et al.*, 2015; Kedersha *et al.*, 2016a; Reineke and Neilson, 2019), yet this question has not been explicitly investigated.

We carried out a screen for SG-inducing molecules (Amen and Kaganovich, 2020c) and found the resveratrol analogue piceatannol among the hits (i.e. inducers of SG formation). Thus, we decided to examine the SG-forming activity of resveratrol together with its natural and synthetic analogs. Here we show that resveratrol, piceatannol, pterostilbene, and 3,4,5,4′-tetramethoxystilbene all induce SG formation at 100–400 μM concentrations (for comparison, red wine contains μM concentrations that vary substantially depending on varietal and growth conditions, since concentrations of stilbenes in plants can increase with stress to reach 100–150 μM; Martinez-Ortega *et al.*, 2000; Poutaraud *et al.*, 2007; Bavaresco *et al.*, 2016). Resveratrol-induced SGs form in human and plant (*A. thaliana*) cells alike, but do not form in yeast, *S. cerevisiae*. Further investigating the dynamics of stilbene-derived SGs, we discovered that SGs formed by resveratrol and piceatannol require at least one isoform of G3BP1 and have unusually rapid clearance kinetics. Resveratrol is known to bind to G3BP1, reducing its valency by displacing its binding partner, USP10 (Buchan *et al.*, 2013; Wheeler *et al.*, 2016; Kaganovich, 2017; Mediani *et al.*, 2021). It is therefore interesting that it produces highly unstable SGs, which in many other aspects resemble SGs formed by conventional stresses such as heat, arsenite, and starvation.

RESULTS

Resveratrol, piceatannol, pterostilbene, and 3,4,5,4′-tetramethoxystilbene induce stress granule formation in human cells

We identified piceatannol in a screen for inducers of PABPC1-positive SG formation (Amen and Kaganovich, 2020c). Piceatannol is a natural stilbenoid, analogous to resveratrol and other stilbene-containing molecules, such as pterostilbene and 3,4,5,4′-tetramethoxystilbene (Figure 1A). To confirm that we observed *bona fide* SGs, we visualized the canonical SG markers G3BP and TIA1 using immunofluorescence. Resveratrol and its analogs induced SG formation at a concentration similar to that of arsenite treatment in HEK293T cells (Figure 1B). We confirmed that resveratrol also induces SGs in different human cell lines, HeLa and U2OS

FIGURE 1: Resveratrol, piceatannol, pterostilbene, and 3,4,5,4′-tetramethoxystilbene induce SG formation. (A) Chemical structure of resveratrol (CID 445154), piceatannol (CID 667639), pterostilbene (CID 5281727), and 3,4,5,4′-tetramethoxystilbene (CID 5388065). (B) Immunofluorescence of SG markers in PABPC1-DDR2 HEK293T cells treated with resveratrol (100 μM), piceatannol (100 μM), pterostilbene (100 μM), 3,4,5,4′-tetramethoxystilbene (100 μM), and arsenite (100 μM) for 1 h. Cells were fixed and stained with anti-TIA1 and anti-G3BP antibodies. Hoechst (10 μg/ml) was used to stain the nucleus 15 min before the imaging. Confocal planes are shown; scale bar 5 μm. (C, D) Confocal microscopy and quantification of SG formation in HEK293T cells expressing endogenously tagged PABPC1-DDR2 during treatment with resveratrol (200 μM), piceatannol (100 μM), pterostilbene (100 μM), 3,4,5,4′-tetramethoxystilbene (100 μM), and arsenite (100 μM) for 1 h, with and without cycloheximide (10 μg/ml, simultaneous addition); scale bar 5 μm. Quantification shows the ratio of cells with SGs in the population, mean ± SEM, $n = 3$ ratios pooled from 300 cells. (E) Western blot of eIF2α phosphorylation on Ser51 in HeLa cell lysates. Cells were treated with resveratrol (Resv, 200 μM), piceatannol (Picea, 100 μM), pterostilbene (Ptero, 100 μM), 3,4,5,4′-tetramethoxystilbene (Tms, 100 μM), and arsenite (Ars, 100μ M) for 1 h before lysis. * $p < 0.01$.

(Supplemental Figure S1, A and B). Cycloheximide is known to block SG formation by inhibiting polysome disassembly (Kedersha *et al.*, 2002; Mollet *et al.*, 2008). Addition of cycloheximide to resveratrol and stilbene derivatives prevented SG formation as with arsenite SGs (Figure 1, C and D). Next, we asked whether resveratrol triggers the integrated stress response by measuring eIF2α phosphorylation at Ser51 (Pakos-Zebrucka *et al.*, 2016; Rabouw *et al.*, 2020), as has been shown for arsenite (Farny *et al.*, 2009). Resveratrol and analogs did not induce a significant increase in eIF2α phosphorylation (Figure 1E; Supplemental Figure S4A).

Resveratrol- and piceatannol-induced stress granules are smaller but show similar formation kinetics

Next, we analyzed the dynamics of SG formation. SGs form as smaller granules, gradually increasing in size by swelling and slowly coalescing (Figure 2A; Wheeler *et al.*, 2016). Although the SGs in resveratrol and arsenite conditions were similar in appearance (Figure 2B; Supplemental Figure S1C), resveratrol-induced SGs showed a higher ratio of smaller to larger granules, significantly decreasing the average size of the SG population, even though larger SGs in the population were of a size similar to that of arsenite SGs (Figure 2C; Supplemental Figure S1D, arrow). Quantification of SG number showed an increase in SGs per cell, compared with arsenite SGs, in response to resveratrol treatment (Supplemental Figure S1D). We next looked at the formation kinetics by plotting the average size of SGs in the population over the time course of SG formation. The formation dynamics of SG under arsenite vs. resveratrol conditions was similar in HEK293T cells, plateauing at 30–40 min of the treatment, except for the difference in the average size of the resulting granules, explained by a higher proportions of smaller initiating clusters under resveratrol and piceatannol conditions (Figure 2, D and E). Next, we measured the internal dynamics of resveratrol and arsenite SGs, using an endogenously tagged PABPC1-Dendra2 cell line (Amen and Kaganovich, 2020b, 2021). Dendra2 is a photoconvertible fluorescent protein (Gurskaya *et al.*, 2006; Chudakov *et al.*, 2007), and the PABPC1–Dendra2 fusion undergoes red-shifted photoconversion upon a pulse exposure to a nonphototoxic dose of a 406-nm laser (Gurskaya *et al.*, 2006; Figure 2F). This enables us to track the photoconverted (red) protein pool in a single SG (Gura Sadovsky *et al.*, 2017; Amen and Kaganovich, 2020b; Figure 2F). When comparing internal dynamics of SGs under arsenite and resveratrol conditions, we measured only SGs that were equivalent in size (larger SGs from resveratrol conditions to match arsenite SGs) due to technical constraints (Amen and Kaganovich, 2020b). In each case we photoconverted a "tail" region of the SG and tracked the photoconverted proteins over time, measuring the intensity profile from photoconverted to nonphotoconverted areas every minute, as was previously described (Figure 2, G—resveratrol, H—arsenite; Amen and Kaganovich, 2020b). The equilibration of photoconverted and nonphotoconverted areas (Supplemental Figure S1, E–F) was considered as complete diffusion (Amen and Kaganovich, 2020a). Resveratrol and arsenite SGs did not show significant differences in their internal dynamics (as measured by PABPC1 diffusion rates in HEK293T cells; Figure 2I). Together these data indicate that resveratrol-induced SGs do not differ significantly from arsenite SGs in the formation kinetics and internal dynamics of PABPC1. Next, we asked how resveratrol might trigger SG formation.

Resveratrol-similar molecules do not induce stress granules

Resveratrol is capable of binding estrogen receptors due to structural similarity to their ligands, thereby activating transcription of estrogen-responsive reporter genes (Gehm *et al.*, 1997). We therefore asked whether estradiol could trigger SG formation. Increasing concentrations of estradiol did not induce SGs (Supplemental Figure S2A). Additionally, we tested p-coumaric acid, the structural precursor of resveratrol (Shin *et al.*, 2011). This compound did not induce the formation of SGs either (Supplemental Figure S2A).

Resveratrol does not induce stress granules in yeast, *Saccharomyces cerevisiae*

Resveratrol has been shown to extend lifespan in a wide range of eukaryotes from yeast to mammals through the activation of sirtuins: conserved NAD-dependent protein deacetylases (Howitz *et al.*, 2003; Wood *et al.*, 2004; Baur *et al.*, 2006; Baur and Sinclair, 2006). Resveratrol activates yeast Sir2 and mammalian SIRT1 and SIRT2 (Howitz *et al.*, 2003; Hou *et al.*, 2016; Pan *et al.*, 2017). We asked whether resveratrol induces SGs in the yeast *Saccharomyces cerevisiae*. Treating yeast cells with increasing concentrations of resveratrol does not induce SG formation in yeast, indicating that sirtuin activation is not a sufficient condition to trigger resveratrol-induced SG formation (Figure 3A).

Resveratrol induces stress granules in *Arabidopsis thaliana* seedlings

Because resveratrol is a natural plant metabolite, we deemed it logical to ask whether exogenous resveratrol also induces SGs in plant cells. We used previously described transgenic seedlings of *A. thaliana* carrying a GFP-tagged SG marker—RNA-binding protein Rbp47b (AT3G19130; Gutierrez-Beltran *et al.*, 2015; Kosmacz *et al.*, 2019); as a control for SG formation we used heat stress (Nover *et al.*, 1989; Weber *et al.*, 2008). Both resveratrol and heat stress induced SGs in the plants (Figure 3B). As a control, we incubated the *A. thaliana* seedlings with cycloheximide, which is known to inhibit SG formation, during resveratrol and heat stress treatments (Kedersha *et al.*, 2002; Kosmacz *et al.*, 2019). Indeed, cycloheximide prevented SG formation under both conditions (Figure 3, C and D), confirming that the inclusions are SGs.

G3BP is required for the formation of resveratrol-induced stress granules

Resveratrol is known to bind the core SG component, Ras-GTPase-activating protein SH3 domain-binding protein 1 (G3BP1; Oi *et al.*, 2015). G3BP is an early SG nucleation factor, forming the intra-SG network of proteins though multivalent interactions of its intrinsically disordered regions with its binding partners (Kedersha *et al.*, 2016; Sanders *et al.*, 2020; Yang *et al.*, 2020). Mammalian cells devoid of both isoforms of G3BP do not form arsenite-induced SGs (Yang *et al.*, 2020). We therefore confirmed that resveratrol-induced SGs do not form in the G3BP1/2 KO cells (Yang *et al.*, 2020; Figure 4A), using another G3BP-binding protein, Caprin1 (Kedersha *et al.*, 2016), as a SG marker. Next, we overexpressed G3BP1 in a double knockout background (G3BP1/2KO) and triggered SG formation with arsenite and resveratrol (S2B). Overexpression of SG components is known to trigger SG formation; however, only 1% of the cells formed SGs when overexpressing one isoform of G3BP in the G3BP1/2 KO background (S2C). Surprisingly, resveratrol induced rodlike SGs (Figure 4, B and C; Supplemental Figure S2D) compared with round arsenite-induced SGs in the KO background. Both conditions induced SGs in a lower percentage of double knockout cells than in the wild-type cells. Resveratrol binding to G3BP1 is known to displace its binding factors; thus it is possible to conclude that the rodlike appearance in the absence of a second G3BP isoform results from a reduced valency of G3BP1 (Figure 4E;

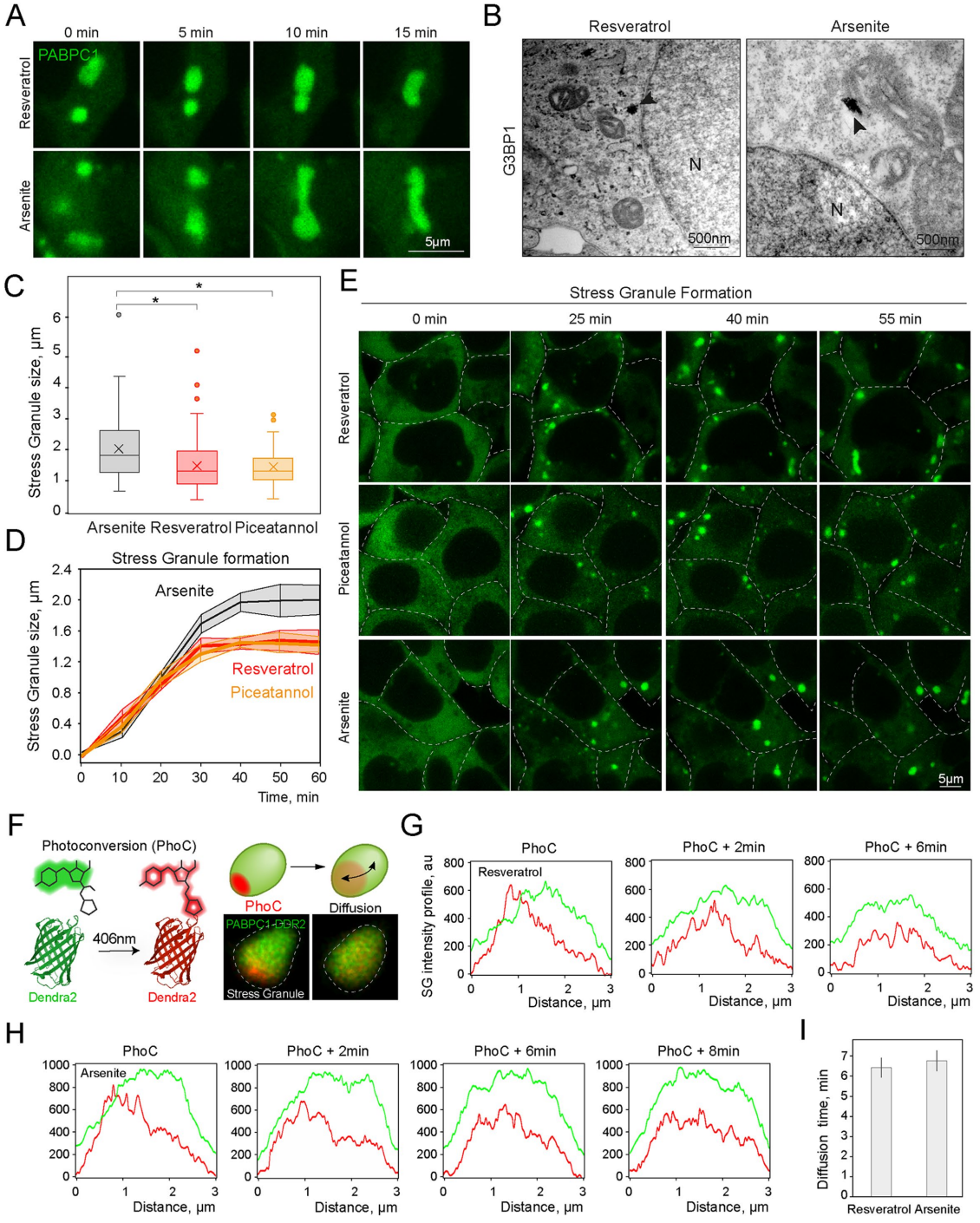

FIGURE 2: Resveratrol- and piceatannol-induced SGs are smaller with similar formation kinetics. (A) Confocal microscopy of SG fusion in HEK293T cells expressing endogenously tagged PABPC1-DDR2 treated with resveratrol (100 μM) and arsenite (100 μM) for 30 min; scale bar 5 μm. (B) Transmission electron microscopy of SGs in SHSY-5Y cells prestained with anti-G3BP gold antibodies. N indicates nuclei; arrowheads indicate SGs; scale bar 500 nm. (C) Quantification of the SG size in the population, box and whisker plot, mean ± SEM, $n = 100$. * $p < 0.05$. Confocal microscopy images were used for the quantification. (D, E) Quantification and confocal microscopy of SG formation in HEK293T cells expressing endogenously tagged PABPC1-DDR2 treated with arsenite (200 μM), piceatannol (200 μM), or resveratrol (200 μM) for indicated amounts of time. D, Line graph shows average SG size change over time, mean ± SEM, $n = 30$ for each time point and treatment. E, Representative confocal images are shown; scale bar 5 μm. (F) Schematic of photoconversion (PhoC) using PABPC1-DDR2. Confocal planes show single SGs in live HEK293T cells expressing CRISPR/Cas9 tagged PABPC1-DDR2 during and after photoconversion. (G, H) Fluorescence intensity profiles of a single SG during photoconversion and diffusion under resveratrol, B, and arsenite conditions, C. Red graphs represent photoconverted DDR2 population. (I) Quantification of the photoconverted PABPC1-DDR2 diffusion time inside single SGs under resveratrol and arsenite conditions; mean ± SEM; $n = 15$; nonsignificant differences.

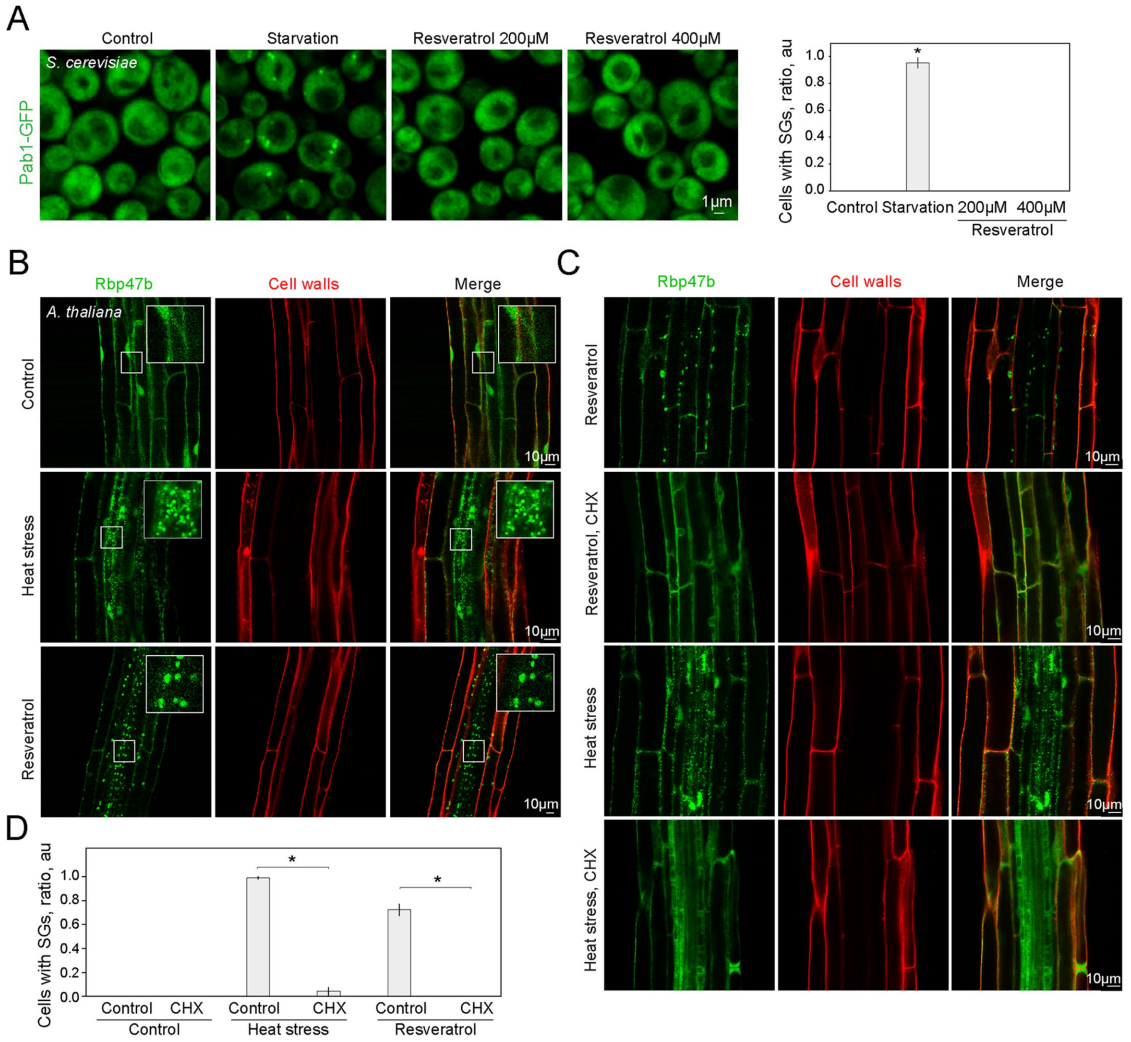

FIGURE 3: Resveratrol induces SGs in *A. thaliana* seedlings. (A) Confocal microscopy of yeast, *S. cerevisiae* expressing endogenously tagged Pab1-GFP SG marker grown to the mid-log phaser and treated with the indicated concentrations of resveratrol, or starved for 1 h; representative images are shown, Quantification shows the proportion of cells with SGs in the population; mean ± SEM; $n = 3$ pooled from 300 cells. * $p < 0.01$. (B) Confocal microscopy of *A. thaliana* root cells expressing GFP-tagged Rbp47b SG marker incubated in the control, heat stress (41°C for 40 min in darkness), or resveratrol (200 μM for 45 min). Representative images are shown; scale bar 10 μm. Cell walls are visualized by propidium iodide staining. (C) Confocal microscopy of *A. thaliana* root cells expressing GFP-tagged Rbp47b SG marker incubated in resveratrol or under heat stress with or without cycloheximide (CHX) for 45 min (CHX 200 ng μl^{-1} was added together with resveratrol). Cell walls are visualized by propidium iodide dye. Representative images are shown; scale bar 10 μm. (D) Quantification shows the ratio of cells with SGs in the population; mean ± SEM; $n = 3$ pooled from 300 cells. * $p < 0.01$.

Soncini *et al.*, 2001). To address this, we targeted the F33 residue of G3BP, which, when mutated to F33W, inhibits G3BP binding to Caprin1 and USP10 (Figure 4B; Panas *et al.*, 2015; Reineke and Lloyd, 2015; Kedersha *et al.*, 2016). Caprin1 displacement was more pronounced in the F33A mutants than in WT G3BP1. Displacement of Caprin1 by resveratrol correlated with reduced levels of SGs compared with arsenite under the same conditions (Figure 4D). It is possible that since Caprin1 promotes SG nucleation, resveratrol displacement of Caprin1 from G3BP has an inhibitory effect on SG formation (Kedersha *et al.*, 2016). However, it is also possible that the F33A mutant has a lower affinity for resveratrol, as well as Caprin1, resulting in a lower rate of SG formation than for arsenite (Figure 4D). To further test whether SG formation stems from resveratrol reducing G3BP valency, we looked at the G3BP-USP10 interaction.

Resveratrol- and piceatannol-induced stress granules clear immediately upon stress removal

The binding of resveratrol to G3BP displaces its binding other partner, USP10 (Oi *et al.*, 2015). USP10 has been shown to inhibit SG nucleation by occupying G3BP (Kedersha *et al.*, 2016). USP10 overexpression blocks arsenite-induced SG formation by binding available G3BP (Kedersha *et al.*, 2016). Interestingly, these studies proposed the possibility of SG formation by resveratrol (Oi *et al.*, 2015; Kedersha *et al.*, 2016). We hypothesized that if resveratrol blocks USP10 from binding G3BP, then overexpression of a USP10 binding fragment will not block resveratrol SGs as it does arsenite SGs. We used a previously described USP10 (1–40) fragment (Kedersha *et al.*, 2016), WT and F10A (mutation that prevents it from binding G3BP; Kedersha *et al.*, 2016). Indeed, the WT USP10 fragment (fused to mCherry) abolished arsenite-induced SGs (Figure 5, A and B),

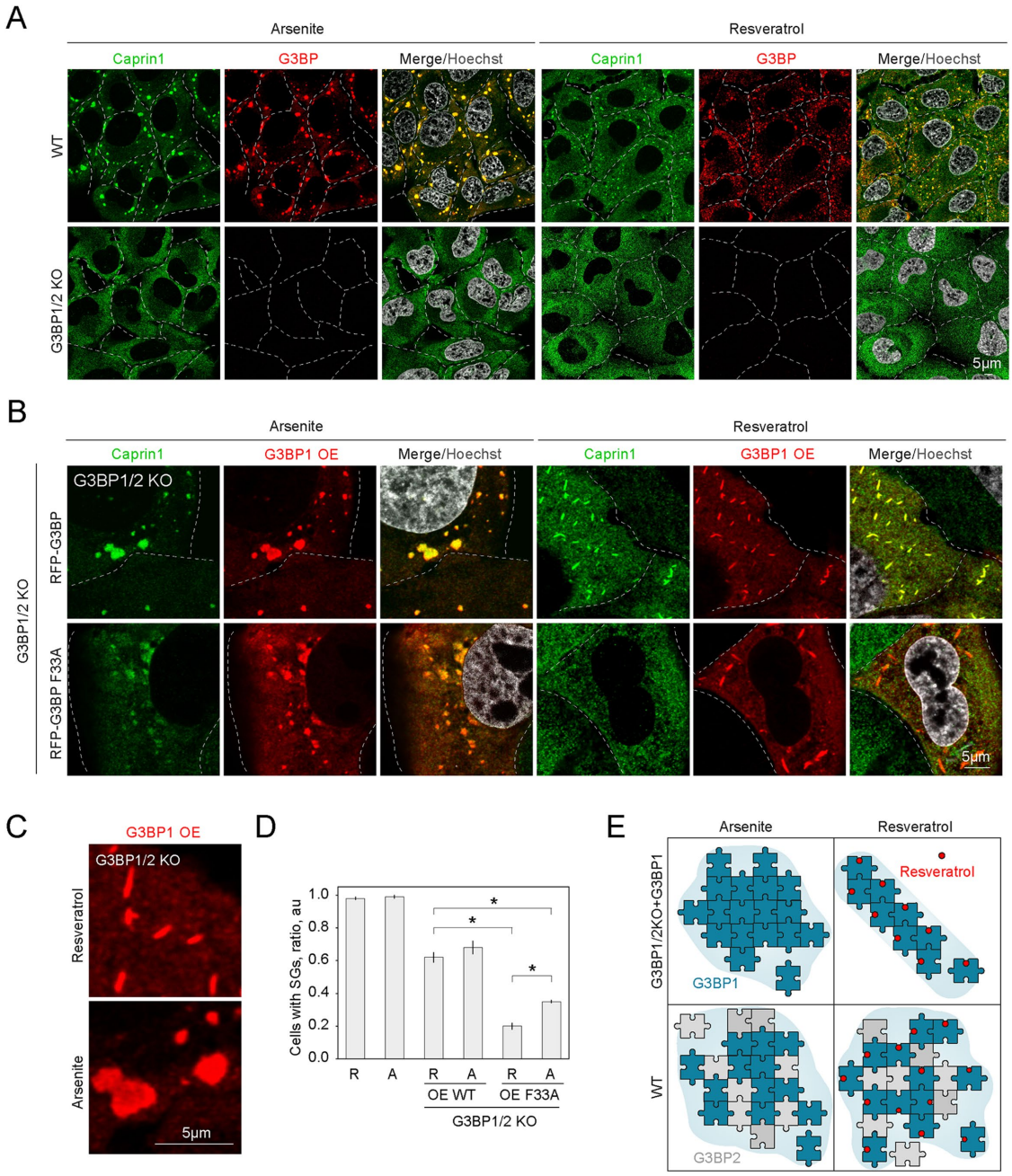

FIGURE 4: G3BP is required for the formation of resveratrol-induced SGs. (A) Confocal microscopy of SG formation in U2OS WT and G3BP1/2 KO cells during treatment with resveratrol (400 μM) and arsenite (400 μM) for 1 h; scale bar 5 μm. (B, C) Confocal microscopy of SG formation in U2OS G3BP1/2 KO cells overexpressing RFP-G3BP1 or RFP-G3BP F33A during treatment with resveratrol (400 μM) and arsenite (400 μM) for 1 h; scale bar 5 μm. (D) Quantification shows the proportion of cells with SGs in the population; mean ± SEM; $n = 3$ ratios pooled from 300 cells for each condition. (E) Model of hypothetical SG formation with a reduced valence of its core nucleating factor.

whereas resveratrol SGs formed in both WT and F10A USP10-mCherry overexpressing cells (Figure 5, A and B). This, in our estimation, confirms the hypothesis that resveratrol competes with USP10 for G3BP binding. Further supporting this, in USP10 fragment-expressing cells treated with resveratrol, we observed an anti-correlation between fragment expression and SG formation—cells with higher USP10 levels formed fewer SGs (Figure 5C).

If USP10 displacement is the mechanism of resveratrol-induced SG formation, then it would follow that SG clearance kinetics should differ from that of arsenite-induced SGs, which are triggered by the integrated stress response and in which G3BP valency is higher, enabling more contacts within the intra-SG protein network (Figure 5F). We measured SG clearance (the process of SG dissolution upon stress removal) by plotting SG size over time after removal of arsenite, resveratrol, or piceatannol. Arsenite recovery induced a gradual 60-min clearance (comparable to the formation kinetics in reverse; Figure 5, D and E). Resveratrol and piceatannol removal, however, induced immediate dissolution of SG components, with complete clearance taking only 5 min in HEK293T cells (Figure 5, D and E). We confirmed this rapid clearance in U2OS cells

(Supplemental Figure S3, A and B). Additionally, clearance of resveratrol SGs was not perturbed by proteasome inhibition (Supplemental Figure S3B), unlike that of arsenite SGs. SGs formed by adding resveratrol and arsenite together did not show a significant difference in clearance from just arsenite SGs (Figure S3C).

DISCUSSION

G3BP is a core SG nucleating component and is therefore essential for SG formation (Tourriere *et al.*, 2003; Yang *et al.*, 2020). G3BP regulates SG assembly and clearance by binding to either Caprin1 or USP10 (Kedersha *et al.*, 2016), which compete for the same binding site. Binding to Caprin1 is thought to promote nucleation, whereas binding to USP10 drives SG clearance (Kedersha *et al.*, 2016). Resveratrol binds the same domain of G3BP as USP10, thus displacing it (Oi *et al.*, 2015). In this study, we show that resveratrol and other stilbene-containing molecules (piceatannol, pterostilbene, and 3,4,5,4′-tetramethoxystilbene) all induce SG formation in mammalian cells, and resveratrol induces SG formation in plants (we did not test other components in plant cells). Overexpressing USP10 (or other proteins containing a FGDF domain) blocks SG formation (Kedersha *et al.*, 2016). Resveratrol-induced SGs form in the presence of overexpressed USP10 (1–40), suggesting that resveratrol induces SG assembly by displacing USP10.

Interestingly, in plants, viral proteins bind G3BP orthologues to prevent SG functioning during infection (Panas *et al.*, 2015; Krapp *et al.*, 2017; Reuper *et al.*, 2021; Reuper and Krenz, 2021). Plants that synthesize stilbene components up-regulate their synthesis during stress and infection (Montero *et al.*, 2003; Hasan and Bae, 2017; Li *et al.*, 2017): it is therefore interesting to speculate that resveratrol binding to G3BP1 counteracts the block on SG formation induced by viral infection, though further investigation is needed to understand the roles of resveratrol, SG formation, and SG clearance in plant stress defense mechanisms. It is clear, however, that resveratrol induces SG formation in plant cells (Figure 3, B and C).

Using photoconversion microscopy of the PABPC1 SG component, we show that resveratrol- and arsenite-induced SGs have similar internal dynamics. We note, however, that the composition of these SGs and the dynamics of other SG components may or may not be similar. For example, resveratrol treatment in mice before SG formation induced by arsenite has been shown to change SG composition, preventing Rbfox2 localization to SGs (Choi *et al.*, 2019).

Resveratrol- and piceatannol-induced SGs exhibit atypically rapid clearance kinetics, disappearing immediately upon resveratrol or piceatannol removal. This suggests a different clearance mechanism from that of the arsenite-induced SGs. Indeed, our data show that resveratrol does not induce phosphorylation of eIF2α to the same extent, which is otherwise a common mechanism of SG nucleation, also triggered by arsenite, because resveratrol drives SG formation even in the presence of overexpressed USP10. Additionally, expressing G3BP F33A as a single isoform in the double knockout background partially reduces binding to Caprin1 and results in a significant reduction of resveratrol-induced SGs, compared with those induced by arsenite. Thus, it is possible that merely displacing USP10, which normally prevents G3BP nucleation, is sufficient to allow resveratrol to trigger SG formation. In this case, however, SGs are less pronounced (a larger portion of smaller SGs is present in resveratrol than in arsenite) since Caprin1, also important for nucleating SGs, is similarly displaced (since USP10 and Caprin1 share the same G3BP binding site; Kedersha *et al.*, 2016). This, in turn, reduces the complexity of the SG network, since G3BP forms fewer bonds, thus allowing SGs to disassemble faster. If this is indeed that case, our model indicates an auxiliary SG-forming pathway that is quicker and more transient than "typical" arsenite-derived SGs. This would enable the investigation of SG assembly in partial isolation from the signaling pathways that are typically involved. It is possible that clearance kinetics depends on the SG assembly pathway: fast-clearing SGs may form in the absence, or with minimal involvement, of eIF2alpha phosphorylation (as we recently demonstrated for fasnall-induced fast clearing SGs; Amen and Kaganovich, 2020a). Additionally, reducing SG complexity or size interferes with eIF2 activation (Reineke *et al.*, 2015); indeed, smaller resveratrol SGs are not able to mount the eIF2 phosphorylation to the same extent as arsenite. On the other hand, resveratrol is known to have many molecular targets, including those regulating SG formation (e.g., mTOR and PKC; Slater *et al.*, 2003; Pirola and Frojdo, 2008; Kulkarni and Canto, 2015; Park *et al.*, 2016). It is therefore possible that G3BP binding is only part of the mechanism regulating SG formation by resveratrol.

In contrast to the mechanisms governing SG formation, the process of SG clearance remains relatively obscure, with a handful of recent studies beginning to investigate this question (Wheeler *et al.*, 2016; Amen and Kaganovich, 2020a; Marmor-Kollet *et al.*, 2020; Hofmann *et al.*, 2021; Mediani *et al.*, 2021). There are a number of reasons for thinking that SG clearance is a key aspect of SG biology. First, persistent SGs have been linked to pathological conditions caused by SG dysfunction, since they have a tendency to undergo aberrant aggregation with many harmful aftereffects (Li *et al.*, 2013; Kroschwald *et al.*, 2015; Patel *et al.*, 2015; Mateju *et al.*, 2017; Maharana *et al.*, 2018). Second, SGs have been shown to carry out important time-sensitive functions during stress, such that the persistence of SGs determines the on/off dynamics of these functions (Takahara and Maeda, 2012; Takahashi *et al.*, 2013; Zhang *et al.*, 2018b; Amen and Kaganovich, 2020d). For example, we recently showed that SGs form on mitochondria during prolonged starvation stress and inhibit the import of fatty acids for fatty acid oxidation (Amen and Kaganovich, 2021). Because SGs formed through other pathways nevertheless have an inhibitory effect on fatty acid oxidation, the SG lifetime as determined by clearance kinetics will have a profound impact on cell metabolism (Amen and Kaganovich, 2021).

MATERIALS AND METHODS

Request a protocol through *Bio-protocol*.

Cell culture and cell lines

HEK293T, U2OS, and HeLa cells were maintained in DMEM supplemented with 10% fetal bovine serum (FBS), 1% penicillin/streptomycin, at 37°C/5% CO_2. SH-SY5Y cells were maintained in 1:1 F12/DMEM media supplemented with 10% FBS, 1% penicillin/streptomycin at 37°C/5% CO2. Construction of CRISPR/Cas9 PABPC1-Dendra2 cell line was described previously (Amen and Kaganovich, 2020b). Cells were transfected using RotiFect transfection reagent (Carl Roth) according to the manufacturer instructions.

We used standard conditions for culturing yeast cells (Sherman, 2002). Yeast Pab1-GFP strain was described previously (Amen and Kaganovich, 2020d).

Stress granule formation in human cells

SGs were induced by treating 80–90% confluent cells with arsenite, resveratrol, or other stilbenes. It is of note that concentration of the drugs needs to be optimized for the cell line (HEK293T cells require 100–200 μM, while U2OS cells require 400–500 μM) and the timing of the experiment (higher concentrations will usually result in a faster SG formation). It is important to note that since resveratrol SGs are very transient, the experiments that require PBS washes should be

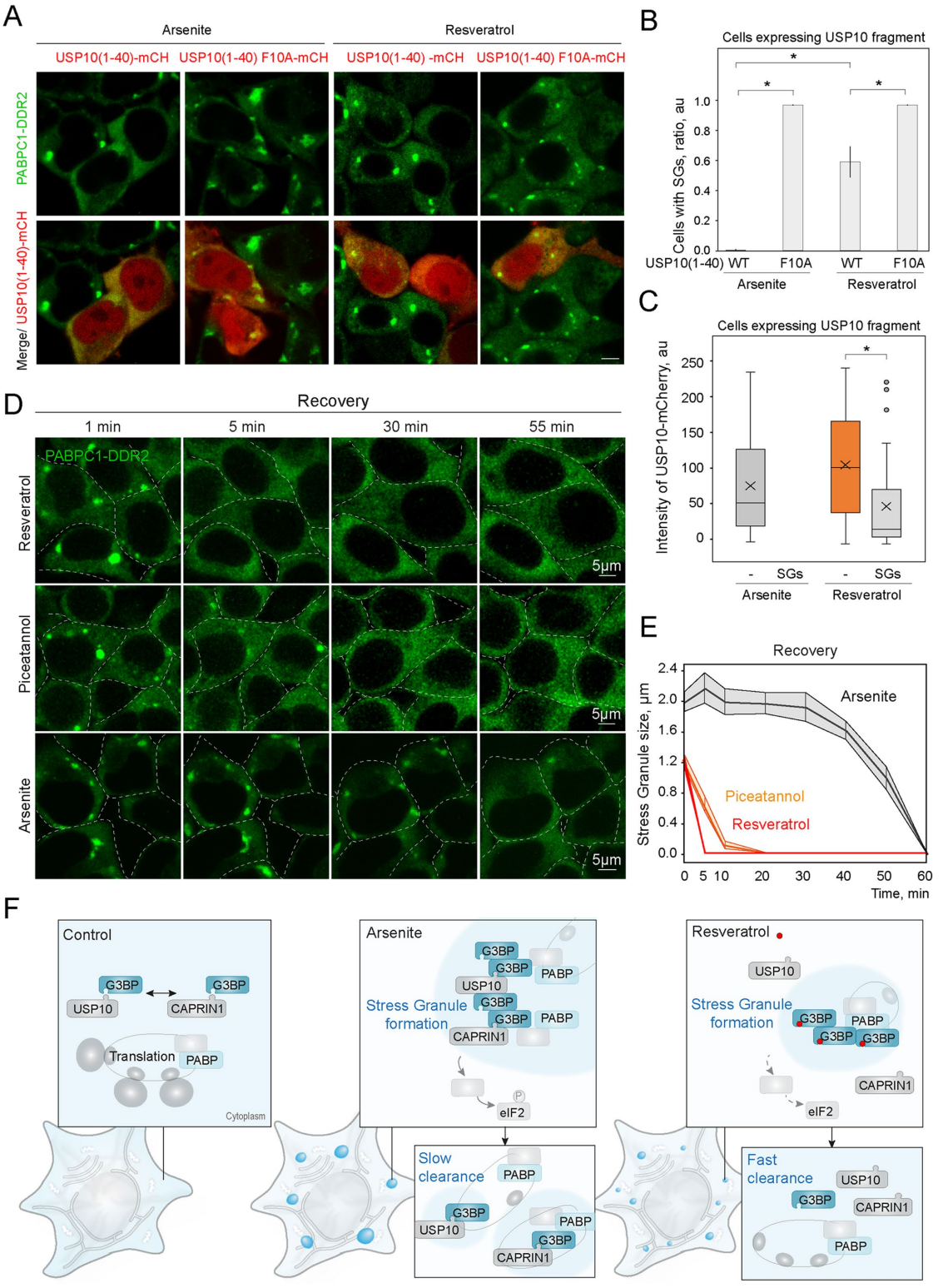

FIGURE 5: Resveratrol- and piceatannol-induced SGs clear immediately upon stress removal. (A, B) Confocal microscopy and quantification of SG formation in HEK293T cells expressing USP10(1-40)-mCherry WT and F10A fragment and CRISPR/Cas9 tagged PABPC1-DDR2 treated with resveratrol (100 μM) or arsenite (100 μM) for 1 h; scale bar 5 μm. Quantification shows the proportion of cells with SGs in the population of cells expressing the constructs; mean ± SEM; $n = 3$ pooled from 300 cells. * $p < 0.01$. (C, D) Quantification and confocal microscopy of SG clearance in HEK293T cells expressing endogenously tagged PABPC1-DDR2 treated with arsenite (200 μM), piceatannol (200 μM), or resveratrol (200 μM) for 1 h, washed three times with PBS, and imaged for 1 h. (E) Model of SG formation and clearance under arsenite and resveratrol conditions. Line graph shows average SG size change over time; mean ± SEM, pooled from at least 100 cells for each time point and treatment. (F) Representative confocal images are shown. Scale bar 5 μm.

done expeditiously, and a higher concentration of resveratrol may be used (200 µM instead of 100 µM). It is of note that resveratrol is not stable in solution; in our hands the potency slowly decreased over a month of storage at –20°C.

The internal dynamics of SGs was assessed as previously described (Amen and Kaganovich, 2020b).

Plant growth conditions and stress granule induction

A. thaliana 35S:GFP–Rbp47b seeds (Gutierrez-Beltran *et al.*, 2015) were sterilized with 70% ethanol, stratified for 2 d at 4°C in the dark, and then germinated vertically at 22°C under continuous light (100 µE) on agar plates containing half-strength Murashige and Skoog (MS) medium (Murashige and Skoog, 1962). The SG induction analyses were performed on 5-day-old seedlings. To induce heat stress SGs, the seedlings were incubated for 40 min in darkness at 41°C. Control seedlings were kept at room temperature (RT). Seedlings were incubated with indicated amounts of resveratrol in 1 ml for 45 min to induce SGs.

Seedlings were analyzed with a Leica Stellaris 5 inverted confocal microscope using a ×63 water immersion objective. For green fluorophore, the following excitation and detection windows were used: 488 nm, 500–530 nm; for propidium iodide dye (for cell walls): 488 nm, 590–650 nm.

Antibodies

We used the following reagents to detect proteins: monoclonal anti-G3BP (Sigma-Aldrich WH0010146M1), polyclonal anti-TIA1 produced in rabbit (Sigma-Aldrich SAB4301803), anti-GAPDH (sc-47724, Santa Cruz Biotechnology), eIF2α (9722, Cell Signaling Technology), Phospho-eIF2α (Ser51; 9721, Cell Signaling Technology).

Secondary antibodies: anti-Rabbit IgG Cy3-conjugated (Sigma-Aldrich C2306), anti-Mouse IgG Cy3-conjugated (Sigma-Aldrich C2181), anti-rabbit IgG Cy5 conjugated (Invitrogen A10523), Goat Anti-Mouse IgG H&L (20 nm Gold) preadsorbed (ab27242).

Chemicals

Hoechst (Sigma), sodium arsenite (Fischer Chemical), cycloheximide (Sigma), DMEM (PAN Biotech), FBS (PAN Biotech), PBS (PAN Biotech), methanol (Roth), aprotinin (Roth), leupeptin (Roth), phenylmethylsulfonyl fluoride (PMSF, Sigma), resveratrol, piceatannol, pterostilbene, 3,4,5,4,'-tetramethoxystilbene, p-coumaric acid, estradiol.

Plasmid Construction

All plasmids were constructed using *Escherichia coli* strain DH5α. Plasmids used in this study are summarized in Table 1.

Microscopy

For live cell imaging we used four-well microscope glass-bottomed plates (IBIDI), or Cellview cell culture dish (Greiner Bio One). Plates were coated with Concanavalin A (Sigma) for live-cell imaging of yeast. Confocal images and movies were acquired using a dual point-scanning Nikon A1R-si microscope equipped with a PInano Piezo stage (MCL) and a temperature and CO_2 incubator, using a 60× PlanApo VC oil objective NA 1.40. We used 406-, 488-, 561-, and 640-nm lasers (Coherent, OBIS). Movies for kymographs were acquired in resonant scanning mode. Image processing was performed using NIS-Elements software.

Electron microscopy

We did preembedding immunogold labeling of SH-SY5Y cells treated with arsenite (200 µM) or resveratrol (200 µM), using monoclonal anti-G3BP (Sigma-Aldrich WH0010146M1) and gold-conjugated secondary antibody (Goat Anti-Mouse IgG H&L; 20 nm Gold; preadsorbed; ab27242; Jones, 2016). The cells were pelleted and fixed with glutaraldehyde, treated with OsO_4, dehydrated, and embedded in epoxy resin following the standard protocol (Jones, 2016). Ultrathin sections were produced with a microtome equipped with a diamond knife, placed on the copper grids, coated with uranyl acetate, and visualized on the transmission electron microscope (Zeiss LEO906E, Germany; (Jones, 2016).

Plasmid name	Source
pcDNA3.1-USP10(40aa)-mCherry	This study
pcDNA3.1-USP10(40aa)-F10A-mCherry	This study
pRFP-G3BP	Kaganovich laboratory
pRFP-G3BP F33A	This study

TABLE 1: Plasmids used in this study.

Statistics and data analysis

Three or more independent experiments were performed to obtain the data. *p* values were calculated by a two-tailed Student's *t* test or one-way ANOVA for samples following normal distribution. Normal distribution of the data was verified using the Shapiro–Wilk test and the equality of variances was verified by Levene's test. Mann–Whitney or Kruskal–Wallis tests were used for experiments when samples did not follow a normal distribution. The sample sizes were not predetermined. Plots were generated using Matplotlib (Hunter, 2007).

Additional data that support the conclusions of this study are available on reasonable request.

ACKNOWLEDGMENTS

We thank Emilio Gutierrez Beltran for the gift of the *A. thaliana* transgenic SG marker line. We thank Pierre Goloubinoff for his advice on plant experiments. We thank J. Paul Taylor for the gift of U2OS G3BP1/2 KO cell line. A.G. was funded by Swiss National Fund Grant CRSK-3_196689.

REFERENCES

Amen T, Kaganovich D (2020a). Fasnall induces atypically transient stress granules independently of FASN inhibition. iScience 23, 101550.

Amen T, Kaganovich D (2020b). Quantitative photoconversion analysis of internal molecular dynamics in stress granules and other membraneless organelles in live cells. STAR Protocols 1, 100217.

Amen T, Kaganovich D (2020c). Small molecule screen reveals joint regulation of stress granule formation and lipid droplet biogenesis. Front Cell Dev Biol 8, 606111.

Amen T, Kaganovich D (2020d). Stress granules sense metabolic stress at the plasma membrane and potentiate recovery by storing active Pkc1. Sci Signal 13, aaz6339.

Amen T, Kaganovich D (2021). Stress granules inhibit fatty acid oxidation by modulating mitochondrial permeability. Cell Rep 35, 109237.

Anderson P, Kedersha N (2006). RNA granules. J Cell Biol 172, 803–808.

Arai D, Kataoka R, Otsuka S, Kawamura M, Maruki-Uchida H, Sai M, Ito T, Nakao Y (2016). Piceatannol is superior to resveratrol in promoting neural stem cell differentiation into astrocytes. Food Funct 7, 4432–4441.

Arimoto K, Fukuda H, Imajoh-Ohmi S, Saito H, Takekawa M (2008). Formation of stress granules inhibits apoptosis by suppressing stress-responsive MAPK pathways. Nat Cell Biol 10, 1324–1332.

Baur JA, Pearson KJ, Price NL, Jamieson HA, Lerin C, Kalra A, Prabhu VV, Allard JS, Lopez-Lluch G, Lewis K, *et al.* (2006). Resveratrol improves health and survival of mice on a high-calorie diet. Nature 444, 337–342.

Baur JA, Sinclair DA (2006). Therapeutic potential of resveratrol: the in vivo evidence. Nat Rev Drug Discov 5, 493–506.

Bavaresco L, Lucini L, Busconi M, Flamini R, De Rosso M (2016). Wine resveratrol: From the ground up. Nutrients 8, 222.

Borra MT, Smith BC, Denu JM (2005). Mechanism of human SIRT1 activation by resveratrol. J Biol Chem 280, 17187–17195.

Buchan JR, Kolaitis RM, Taylor JP, Parker R (2013). Eukaryotic stress granules are cleared by autophagy and Cdc48/VCP function. Cell 153, 1461–1474.
Buchan JR, Yoon JH, Parker R (2011). Stress-specific composition, assembly and kinetics of stress granules in *Saccharomyces cerevisiae*. J Cell Sci 124, 228–239.
Choi S, Sa M, Cho N, Kim KK, Park SH (2019). Rbfox2 dissociation from stress granules suppresses cancer progression. Exp Mol Med 51, 1–12.
Chudakov DM, Lukyanov S, Lukyanov KA (2007). Tracking intracellular protein movements using photoswitchable fluorescent proteins PS-CFP2 and Dendra2. Nat Protoc 2, 2024–2032.
Cirillo L, Cieren A, Barbieri S, Khong A, Schwager F, Parker R, Gotta M (2020). UBAP2L forms distinct cores that act in nucleating stress granules upstream of G3BP1. Curr Biol 30, 698–707.e696.
Dusek J, Skoda J, Holas O, Horvatova A, Smutny T, Linhartova L, Hirsova P, Kucera O, Micuda S, Braeuning A, Pavek P (2019). Stilbene compound trans-3,4,5,4 -tetramethoxystilbene, a potential anticancer drug, regulates constitutive androstane receptor (Car) target genes, but does not possess proliferative activity in mouse liver. Toxicol Lett 313, 1–10.
Fan XX, Yao XJ, Xu SW, Wong VK, He JX, Ding J, Xue WW, Mujtaba T, Michelangeli F, Huang M, *et al*. (2015). (Z)3,4,5,4′-trans-tetramethoxystilbene, a new analogue of resveratrol, inhibits gefitinb-resistant non-small cell lung cancer via selectively elevating intracellular calcium level. Sci Rep 5, 16348.
Farny NG, Kedersha NL, Silver PA (2009). Metazoan stress granule assembly is mediated by P-eIF2alpha-dependent and -independent mechanisms. RNA 15, 1814–1821.
Fournier MJ, Coudert L, Mellaoui S, Adjibade P, Gareau C, Cote MF, Sonenberg N, Gaudreault RC, Mazroui R (2013). Inactivation of the mTORC1-eukaryotic translation initiation factor 4E pathway alters stress granule formation. Mol Cell Biol 33, 2285–2301.
Geahlen RL, McLaughlin JL (1989). Piceatannol (3,4,3′,5′-tetrahydroxy-trans-stilbene) is a naturally occurring protein–tyrosine kinase inhibitor. Biochem Biophys Res Commun 165, 241–245.
Gehm BD, McAndrews JM, Chien PY, Jameson JL. (1997). Resveratrol, a polyphenolic compound found in grapes and wine, is an agonist for the estrogen receptor. Proc Natl Acad Sci USA 94, 14138–14143.
Gura Sadovsky R, Brielle S, Kaganovich D, England JL. (2017). Measurement of rapid protein diffusion in the cytoplasm by photo-converted intensity profile expansion. Cell Rep 18, 2795–2806.
Gurskaya NG, Verkhusha VV, Shcheglov AS, Staroverov DB, Chepurnykh TV, Fradkov AF, Lukyanov S, Lukyanov KA (2006). Engineering of a monomeric green-to-red photoactivatable fluorescent protein induced by blue light. Nat Biotechnol 24, 461–465.
Gutierrez-Beltran E, Moschou PN, Smertenko AP, Bozhkov PV (2015). Tudor staphylococcal nuclease links formation of stress granules and processing bodies with mRNA catabolism in *Arabidopsis*. Plant Cell 27, 926–943.
Hasan M, Bae H (2017). An overview of stress-induced resveratrol synthesis in grapes: perspectives for resveratrol-enriched grape products. Molecules 22, 22020294.
Hofmann S, Kedersha N, Anderson P, Ivanov P (2021). Molecular mechanisms of stress granule assembly and disassembly. Biochim Biophys Acta Mol Cell Res 1868, 118876.
Hou X, Rooklin D, Fang H, Zhang Y (2016). Resveratrol serves as a protein–substrate interaction stabilizer in human SIRT1 activation. Sci Rep 6, 38186.
Howitz KT, Bitterman KJ, Cohen HY, Lamming DW, Lavu S, Wood JG, Zipkin RE, Chung P, Kisielewski A, Zhang LL, *et al*. (2003). Small molecule activators of sirtuins extend *Saccharomyces cerevisiae* lifespan. Nature 425, 191–196.
Hunter JD (2007). Matplotlib: a 2D graphics environment. Comput Sci Eng 9, 90–95.
Inoue H, Jiang XF, Katayama T, Osada S, Umesono K, Namura S (2003). Brain protection by resveratrol and fenofibrate against stroke requires peroxisome proliferator-activated receptor alpha in mice. Neurosci Lett 352, 203–206.
Jevtov I, Zacharogianni M, van Oorschot MM, van Zadelhoff G, Aguilera-Gomez A, Vuillez I, Braakman I, Hafen E, Stocker H, Rabouille C (2015). TORC2 mediates the heat stress response in *Drosophila* by promoting the formation of stress granules. J Cell Sci 128, 2497–2508.
Jones JC (2016). Pre- and post-embedding immunogold labeling of tissue sections. Methods Mol Biol 1474, 291–307.
Kaganovich D (2017). There is an inclusion for that: material properties of protein granules provide a platform for building diverse cellular functions. Trends Biochem Sci 42, 765–776.
Kedersha N, Anderson P. (2007). Mammalian stress granules and processing bodies. Methods Enzymol 431, 61–81.
Kedersha N, Chen S, Gilks N, Li W, Miller IJ, Stahl J, Anderson P. (2002). Evidence that ternary complex (eIF2-GTP-tRNA(i)(Met))-deficient preinitiation complexes are core constituents of mammalian stress granules. Mol Biol Cell 13, 195–210.
Kedersha N, Ivanov P, Anderson P. (2013). Stress granules and cell signaling: more than just a passing phase? Trends Biochem Sci 38, 494–506.
Kedersha N, Panas MD, Achorn CA, Lyons S, Tisdale S, Hickman T, Thomas M, Lieberman J, McInerney GM, Ivanov P, Anderson P. (2016). G3BP–Caprin1–USP10 complexes mediate stress granule condensation and associate with 40S subunits. J Cell Biol 212, 845–860.
Kedersha N, Stoecklin G, Ayodele M, Yacono P, Lykke-Andersen J, Fritzler MJ, Scheuner D, Kaufman RJ, Golan DE, Anderson P. (2005). Stress granules and processing bodies are dynamically linked sites of mRNP remodeling. J Cell Biol 169, 871–884.
Khong A, Matheny T, Jain S, Mitchell SF, Wheeler JR, Parker R (2017). The stress granule transcriptome reveals principles of mRNA accumulation in stress granules. Mol Cell 68, 808–820 e805.
Kim S, Ko H, Park JE, Jung S, Lee SK, Chun YJ (2002). Design, synthesis, and discovery of novel trans-stilbene analogues as potent and selective human cytochrome P450 1B1 inhibitors. J Med Chem 45, 160–164.
Kobayashi T, Winslow S, Sunesson L, Hellman U, Larsson C (2012). PK-Calpha binds G3BP2 and regulates stress granule formation following cellular stress. PLoS One 7, e35820.
Kosmacz M, Gorka M, Schmidt S, Luzarowski M, Moreno JC, Szlachetko J, Leniak E, Sokolowska EM, Sofroni K, Schnittger A, Skirycz A (2019). Protein and metabolite composition of *Arabidopsis* stress granules. New Phytol 222, 1420–1433.
Krapp S, Greiner E, Amin B, Sonnewald U, Krenz B (2017). The stress granule component G3BP is a novel interaction partner for the nuclear shuttle proteins of the nanovirus pea necrotic yellow dwarf virus and geminivirus abutilon mosaic virus. Virus Res 227, 6–14.
Kroschwald S, Maharana S, Mateju D, Malinovska L, Nuske E, Poser I, Richter D, Alberti S. (2015). Promiscuous interactions and protein disaggregases determine the material state of stress-inducible RNP granules. Elife 4, e06807.
Kulkarni SS, Canto C (2015). The molecular targets of resveratrol. Biochim Biophys Acta 1852, 1114–1123.
Li R, Xie X, Ma F, Wang D, Wang L, Zhang J, Xu Y, Wang X, Zhang C, Wang Y. (2017). Resveratrol accumulation and its involvement in stilbene synthetic pathway of Chinese wild grapes during berry development using quantitative proteome analysis. Sci Rep 7, 9295.
Li YR, King OD, Shorter J, Gitler AD (2013). Stress granules as crucibles of ALS pathogenesis. J Cell Biol 201, 361–372.
Lim YRI, Preshaw PM, Lim LP, Ong MMA, Lin HS, Tan KS (2020). Pterostilbene complexed with cyclodextrin exerts antimicrobial and anti-inflammatory effects. Sci Rep 10, 9072.
Maharana S, Wang J, Papadopoulos DK, Richter D, Pozniakovsky A, Poser I, Bickle M, Rizk S, Guillen-Boixet J, Franzmann TM, *et al*. (2018). RNA buffers the phase separation behavior of prion-like RNA binding proteins. Science 360, 918–921.
Mann JR, Gleixner AM, Mauna JC, Gomes E, DeChellis-Marks MR, Needham PG, Copley KE, Hurtle B, Portz B, Pyles NJ, *et al*. (2019). RNA binding antagonizes neurotoxic phase transitions of TDP-43. Neuron 102, 321–338.e328.
Markmiller S, Soltanieh S, Server KL, Mak R, Jin W, Fang MY, Luo EC, Krach F, Yang D, Sen A, *et al*. (2018). Context-dependent and disease-specific diversity in protein interactions within stress granules. Cell 172, 590–604.e513.
Marmor-Kollet H, Siany A, Kedersha N, Knafo N, Rivkin N, Danino YM, Moens TG, Olender T, Sheban D, Cohen N, *et al*. (2020). Spatiotemporal proteomic analysis of stress granule disassembly using APEX reveals regulation by SUMOylation and links to ALS pathogenesis. Mol Cell 80, 876–891.e876.
Martinez-Ortega MV, Carcia-Parrilla MC, Troncoso AM (2000). Resveratrol content in wines and musts from the south of Spain. Nahrung 44, 253–256.
Mateju D, Franzmann TM, Patel A, Kopach A, Boczek EE, Maharana S, Lee HO, Carra S, Hyman AA, Alberti S. (2017). An aberrant phase transition of stress granules triggered by misfolded protein and prevented by chaperone function. EMBO J 36, 1669–1687.
McCormack D, McFadden D. (2013). A review of pterostilbene antioxidant activity and disease modification. Oxid Med Cell Longev 2013, 575482.
McGurk L, Gomes E, Guo L, Mojsilovic-Petrovic J, Tran V, Kalb RG, Shorter J, Bonini NM (2018). Poly(ADP-Ribose) prevents pathological phase separation of TDP-43 by promoting liquid demixing and stress granule localization. Mol Cell 71, 703–717.e709.

Mediani L, Antoniani F, Galli V, Vinet J, Carra AD, Bigi I, Tripathy V, Tiago T, Cimino M, Leo G, *et al.* (2021). Hsp90-mediated regulation of DYRK3 couples stress granule disassembly and growth via mTORC1 signaling. EMBO Rep 22, e51740.

Mollet S, Cougot N, Wilczynska A, Dautry F, Kress M, Bertrand E, Weil D. (2008). Translationally repressed mRNA transiently cycles through stress granules during stress. Mol Biol Cell 19, 4469–4479.

Montero C, Cristescu SM, Jimenez JB, Orea JM, te Lintel Hekkert S, Harren FJ, Gonzalez Urena A (2003). trans-Resveratrol and grape disease resistance. A dynamical study by high-resolution laser-based techniques. Plant Physiol 131, 129–138.

Moutaoufik MT, El Fatimy R, Nassour H, Gareau C, Lang J, Tanguay RM, Mazroui R, Khandjian EW (2014). UVC-induced stress granules in mammalian cells. PLoS One 9, e112742.

Murashige T, Skoog F (1962). A revised medium for rapid growth and bio assays with tobacco tissue cultures. Physiol Plantarum 15, 473–497.

Nover L, Scharf KD, Neumann D. (1989). Cytoplasmic heat shock granules are formed from precursor particles and are associated with a specific set of mRNAs. Mol Cell Biol 9, 1298–1308.

Oi N, Yuan J, Malakhova M, Luo K, Li Y, Ryu J, Zhang L, Bode AM, Xu Z, Li Y, *et al.* (2015). Resveratrol induces apoptosis by directly targeting Ras-GTPase-activating protein SH3 domain-binding protein 1. Oncogene 34, 2660–2671.

Pakos-Zebrucka K, Koryga I, Mnich K, Ljujic M, Samali A, Gorman AM (2016). The integrated stress response. EMBO Rep 17, 1374–1395.

Pan Y, Zhang H, Zheng Y, Zhou J, Yuan J, Yu Y, Wang J. (2017). Resveratrol exerts antioxidant effects by activating SIRT2 to deacetylate Prx1. Biochemistry 56, 6325–6328.

Panas MD, Ivanov P, Anderson P. (2016). Mechanistic insights into mammalian stress granule dynamics. J Cell Biol 215, 313–323.

Panas MD, Schulte T, Thaa B, Sandalova T, Kedersha N, Achour A, McInerney GM (2015). Viral and cellular proteins containing FGDF motifs bind G3BP to block stress granule formation. PLoS Pathog 11, e1004659.

Park D, Jeong H, Lee MN, Koh A, Kwon O, Yang YR, Noh J, Suh PG, Park H, Ryu SH (2016). Resveratrol induces autophagy by directly inhibiting mTOR through ATP competition. Sci Rep 6, 21772.

Patel A, Lee HO, Jawerth L, Maharana S, Jahnel M, Hein MY, Stoynov S, Mahamid J, Saha S, Franzmann TM, *et al.* (2015). A liquid-to-solid phase transition of the ALS protein FUS accelerated by disease mutation. Cell 162, 1066–1077.

Piotrowska J, Hansen SJ, Park N, Jamka K, Sarnow P, Gustin KE (2010). Stable formation of compositionally unique stress granules in virus-infected cells. J Virol 84, 3654–3665.

Pirola L, Frojdo S (2008). Resveratrol: one molecule, many targets. IUBMB Life 60, 323–332.

Potter GA, Patterson LH, Wanogho E, Perry PJ, Butler PC, Ijaz T, Ruparelia KC, Lamb JH, Farmer PB, Stanley LA, Burke MD (2002). The cancer preventative agent resveratrol is converted to the anticancer agent piceatannol by the cytochrome P450 enzyme CYP1B1. Br J Cancer 86, 774–778.

Poutaraud A, Latouche G, Martins S, Meyer S, Merdinoglu D, Cerovic ZG (2007). Fast and local assessment of stilbene content in grapevine leaf by in vivo fluorometry. J Agric Food Chem 55, 4913–4920.

Rabouw HH, Visser LJ, Passchier TC, Langereis MA, Liu F, Giansanti P, van Vliet ALW, Dekker JG, van der Grein SG, Saucedo JG, *et al.* (2020). Inhibition of the integrated stress response by viral proteins that block p-eIF2-eIF2B association. Nat Microbiol, https://10.1038/s41564-020-0759-0.

Reineke LC, Cheema SA, Dubrulle J, Neilson JR (2018). Chronic starvation induces noncanonical pro-death stress granules. J Cell Sci 131, 220244.

Reineke LC, Kedersha N, Langereis MA, van Kuppeveld FJ, Lloyd RE (2015). Stress granules regulate double-stranded RNA-dependent protein kinase activation through a complex containing G3BP1 and Caprin1. mBio 6, e02486.

Reineke LC, Lloyd RE (2015). The stress granule protein G3BP1 recruits protein kinase R to promote multiple innate immune antiviral responses. J Virol 89, 2575–2589.

Reineke LC, Neilson JR (2019). Differences between acute and chronic stress granules, and how these differences may impact function in human disease. Biochem Pharmacol 162, 123–131.

Reuper H, Amari K, Krenz B (2021). Analyzing the G3BP-like gene family of *Arabidopsis thaliana* in early turnip mosaic virus infection. Sci Rep 11, 2187.

Reuper H, Krenz B (2021). Comparison of two turnip mosaic virus P1 proteins in their ability to co-localize with the *Arabidopsis thaliana* G3BP-2 protein. Virus Genes 57, 233–237.

Rimando AM, Kalt W, Magee JB, Dewey J, Ballington JR (2004). Resveratrol, pterostilbene, and piceatannol in vaccinium berries. J Agric Food Chem 52, 4713–4719.

Robb EL, Stuart JA (2014). The stilbenes resveratrol, pterostilbene and piceid affect growth and stress resistance in mammalian cells via a mechanism requiring estrogen receptor beta and the induction of Mn-superoxide dismutase. Phytochemistry 98, 164–173.

Sanders DW, Kedersha N, Lee DSW, Strom AR, Drake V, Riback JA, Bracha D, Eeftens JM, Iwanicki A, Wang A, *et al.* (2020). Competing protein–RNA interaction networks control multiphase intracellular organization. Cell 181, 306–324 e328.

Schmidlin L, Poutaraud A, Claudel P, Mestre P, Prado E, Santos-Rosa M, Wiedemann-Merdinoglu S, Karst F, Merdinoglu D, Hugueney P (2008). A stress-inducible resveratrol O-methyltransferase involved in the biosynthesis of pterostilbene in grapevine. Plant Physiol 148, 1630–1639.

Sfakianos AP, Mellor LE, Pang YF, Kritsiligkou P, Needs H, Abou-Hamdan H, Desaubry L, Poulin GB, Ashe MP, Whitmarsh AJ (2018). The mTOR-S6 kinase pathway promotes stress granule assembly. Cell Death Differ 25, 1766–1780.

Sherman F (2002). Getting started with yeast. Methods Enzymol 350, 3–41.

Shin SY, Han NS, Park YC, Kim MD, Seo JH (2011). Production of resveratrol from p-coumaric acid in recombinant *Saccharomyces cerevisiae* expressing 4-coumarate:coenzyme A ligase and stilbene synthase genes. Enzyme Microb Technol 48, 48–53.

Slater SJ, Seiz JL, Cook AC, Stagliano BA, Buzas CJ (2003). Inhibition of protein kinase C by resveratrol. Biochim Biophys Acta 1637, 59–69.

Soncini C, Berdo I, Draetta G (2001). Ras-GAP SH3 domain binding protein (G3BP) is a modulator of USP10, a novel human ubiquitin specific protease. Oncogene 20, 3869–3879.

Stewart JR, Ward NE, Ioannides CG, O'Brian CA. (1999). Resveratrol preferentially inhibits protein kinase C-catalyzed phosphorylation of a cofactor-independent, arginine-rich protein substrate by a novel mechanism. Biochemistry 38, 13244–13251.

Takahara T, Maeda T (2012). Transient sequestration of TORC1 into stress granules during heat stress. Mol Cell 47, 242–252.

Takahashi M, Higuchi M, Matsuki H, Yoshita M, Ohsawa T, Oie M, Fujii M (2013). Stress granules inhibit apoptosis by reducing reactive oxygen species production. Mol Cell Biol 33, 815–829.

Thedieck K, Holzwarth B, Prentzell MT, Boehlke C, Klasener K, Ruf S, Sonntag AG, Maerz L, Grellscheid SN, Kremmer E, *et al.* (2013). Inhibition of mTORC1 by astrin and stress granules prevents apoptosis in cancer cells. Cell 154, 859–874.

Tourriere H, Chebli K, Zekri L, Courselaud B, Blanchard JM, Bertrand E, Tazi J (2003). The RasGAP-associated endoribonuclease G3BP assembles stress granules. J Cell Biol 160, 823–831.

Tsai HY, Ho CT, Chen YK (2017). Biological actions and molecular effects of resveratrol, pterostilbene, and 3'-hydroxypterostilbene. J Food Drug Anal 25, 134–147.

Walker AK, Soo KY, Sundaramoorthy V, Parakh S, Ma Y, Farg MA, Wallace RH, Crouch PJ, Turner BJ, Horne MK, Atkin JD (2013). ALS-associated TDP-43 induces endoplasmic reticulum stress, which drives cytoplasmic TDP-43 accumulation and stress granule formation. PLoS One 8, e81170.

Weber C, Nover L, Fauth M (2008). Plant stress granules and mRNA processing bodies are distinct from heat stress granules. Plant J 56, 517–530.

Wheeler JR, Matheny T, Jain S, Abrisch R, Parker R (2016). Distinct stages in stress granule assembly and disassembly. eLife 5, 18413.

Wieder T, Prokop A, Bagci B, Essmann F, Bernicke D, Schulze-Osthoff K, Dorken B, Schmalz HG, Daniel PT, Henze G (2001). Piceatannol, a hydroxylated analog of the chemopreventive agent resveratrol, is a potent inducer of apoptosis in the lymphoma cell line BJAB and in primary, leukemic lymphoblasts. Leukemia 15, 1735–1742.

Wood JG, Rogina B, Lavu S, Howitz K, Helfand SL, Tatar M, Sinclair D. (2004). Sirtuin activators mimic caloric restriction and delay ageing in metazoans. Nature 430, 686–689.

Yang P, Mathieu C, Kolaitis RM, Zhang P, Messing J, Yurtsever U, Yang Z, Wu J, Li Y, Pan Q, *et al.* (2020). G3BP1 is a tunable switch that triggers phase separation to assemble stress granules. Cell 181, 325–345.e328.

Zhang K, Daigle JG, Cunningham KM, Coyne AN, Ruan K, Grima JC, Bowen KE, Wadhwa H, Yang P, Rigo F, *et al.* (2018a). Stress granule assembly disrupts nucleocytoplasmic transport. Cell 173, 958–971.e917.

Zhang K, Daigle JG, Cunningham KM, Coyne AN, Ruan K, Grima JC, Bowen KE, Wadhwa H, Yang P, Rigo F, *et al.* (2018b). Stress granule assembly disrupts nucleocytoplasmic transport. Cell 173, 958–971.e917.